



CHORUS

This is the accepted manuscript made available via CHORUS. The article has been published as:

Vortex coalescence and type-1.5 superconductivity in $\text{Sr}_{2}\text{RuO}_{4}$

Julien Garaud, Daniel F. Agterberg, and Egor Babaev
Phys. Rev. B **86**, 060513 — Published 29 August 2012

DOI: [10.1103/PhysRevB.86.060513](https://doi.org/10.1103/PhysRevB.86.060513)

Vortex coalescence and type-1.5 superconductivity in Sr_2RuO_4

Julien Garaud^{1,2}, Daniel F. Agterberg³, Egor Babaev^{1,2}

¹*Department of Physics, University of Massachusetts Amherst, MA 01003 USA*

²*Department of Theoretical Physics, The Royal Institute of Technology, Stockholm, SE-10691 Sweden*

³*Department of Physics, University of Wisconsin-Milwaukee, Milwaukee, WI 53211, USA*

Recently vortex coalescence was reported in superconducting Sr_2RuO_4 by several experimental groups for fields applied along the c -axis. We argue that Sr_2RuO_4 is a type-1.5 superconductor with long-range attractive, short-range repulsive intervortex interaction. The type-1.5 behavior stems from an interplay of the two orbital degrees of freedom describing this chiral superconductor together with the multiband nature of the superconductivity. These multiple degrees of freedom give rise to multiple coherence lengths, some of which are larger and some smaller than the magnetic field penetration length, resulting in nonmonotonic intervortex forces.

PACS numbers: 74.20.De, 74.25.Ha, 74.70.Pq

The superconducting state of strontium ruthenate is of great interest because of experimental evidence that it is a chiral spin-triplet superconductor. Support for this point of view came through a variety of measurements that include: the complete suppression of the superconducting transition temperature (T_c) with non-magnetic impurities;¹ NMR Knight shift measurements that show no change in the spin susceptibility with temperature in the superconducting phase;^{2,3} muon spin measurements (μSR) that suggest broken time-reversal symmetry in the superconducting state;⁴ polar Kerr effect showing the broken time-reversal symmetry and the presence of chirality in the superconducting phase;⁵ and phase sensitive measurements consistent with a chiral spin-triplet state.^{6,7} While these measurements provide a strong case for a chiral spin-triplet superconducting phase, the case is not iron clad. In particular, sizable edge currents are expected to flow at sample boundaries and at domain walls between domains of opposite chirality.⁸ A search for these currents has been carried out and they have not been observed.^{9–11} Additionally, for fields in the basal plane, two superconducting phases are predicted¹² and the corresponding phase transition between these phases has also not been observed. Finally, if spin-orbit coupling is sufficiently large, then the spin susceptibility should show no change for fields in the basal plane, but is expected to decrease with temperature for fields along the c -axis. NMR data shows no change on the spin susceptibility for fields both in the basal plane² and along the c -axis.³ In spite of these puzzles in interpreting the superconducting state as a chiral spin-triplet superconductor, the evidence in support of this state remains strong and current research is focused on addressing these puzzles within this framework.

Another interesting aspect of the Sr_2RuO_4 is the multiband nature of its superconductivity. The Fermi surface of Sr_2RuO_4 contains three sheets of cylindrical topology labeled α , β , and γ .¹³ These sheets stem from Ru d_{xz} , d_{yz} and Ru d_{xy} orbitals. In particular, the α and β sheets originate from the d_{xz} and d_{yz} orbitals which lead to quasi-one-dimensional bands, and the γ sheet originates from the d_{xy} orbitals which leads to a quasi-two-

dimensional band. It has been shown that for any non s -wave pairing state, the superconducting order on the γ sheet is weakly coupled to that on the α , β sheets.^{14–16} This enables the physical picture of a multi gap superconductor, where a full gap exists on the active band (either the γ or the α , β bands) and the gap on the passive band is driven by the active gap through the weak coupling between the two gaps. The gap on the passive band may or may not contain nodes depending upon the details of the coupling between the two bands.^{14,15} This scenario is supported by the evolution of the specific heat with magnetic field where it is seen that a small magnetic field is sufficient to remove the gap in passive band.¹⁷ The identification of the active band has been a matter of debate. Specific heat measurements suggest that it is the γ band.¹⁷ However, it has been recently argued that if the α , β bands are the active band, then it is possible that the edge currents are not large,^{18,19} which provides a reason for why they have not been observed (note that small edge currents may make it difficult to explain the fields seen by μSR measurements²⁰). Furthermore, unlike the γ band, superconductivity in the α , β bands gives rise to an intrinsic Hall effect that naturally accounts for the observed polar Kerr effect.²¹

A striking feature which has been repeatedly observed in this material and is the subject of this paper, is vortex coalescence into clusters in various samples.^{9,10,22,23} The experimental works Refs. 9, 10, 22 interpreted this as originating from attractive intervortex interactions of unknown nature. Indeed the mechanisms for possible small intervortex attractions in single-component superconductors cannot apply for this material. In single-component systems vortices have either purely repulsive (in type-2 case) or purely attractive (in type-1 case) interaction at the level of Ginzburg-Landau theory. The situation can be more complex in microscopic models of weak-coupling type-2 superconductors with the Ginzburg-Landau parameter κ extremely close to the Bogomolnyi limit $1/\sqrt{2}$. There, intervortex forces in Ginzburg-Landau theory are vanishingly small. The long-range intervortex forces are then determined by non-universal microscopic physics, which for certain materials can lead to tiny attractive

forces²⁴ which at long range can win over repulsive interaction. However this mechanism can be ruled out in the case of Sr_2RuO_4 since the measurements of critical fields suggest that an estimate for a putative Ginzburg–Landau parameter is too far outside the regime where these effects takes place: $\kappa \approx 2.6$ (see *e.g.* Ref. 10). There exists a different mechanism for intervortex attraction specific for multicomponent systems. Multicomponent superconductors can have several coherence lengths ξ_a . In this case, the intervortex interaction can be long-range attractive and short-range repulsive because of the interplay of the multiple fundamental length scales of the theory. That is, a nonmonotonic interaction occurs if the London penetration length λ falls between the coherence lengths $\xi_1 < \lambda < \xi_2$.^{25–32} This regime was recently termed “type-1.5” superconductivity²⁸ since it features coexisting and competing type-I and type-II behaviors. The nonmonotonic intervortex forces originate there from the “double-core” structure of vortices due to multiple coherence lengths. The outer core (roughly speaking associated to the length scale ξ_2) extends outside the flux carrying area. The overlap of the outer cores of vortices is responsible for the attractive intervortex forces. Yet in the type-1.5 regime the vortices have short range repulsion (due to current-current and electromagnetic interaction) and are thermodynamically stable.²⁵ This should lead to vortex cluster formation in low magnetic field. Here we examine the role of the multiple superconducting degrees of freedom that exist in Sr_2RuO_4 . After it was suggested in Ref. 28 that type-1.5 regime is realized in MgB_2 , a question was raised in the recent experimental work on Sr_2RuO_4 ¹⁰ whether or not the vortex coalescence in Sr_2RuO_4 originates via a type-1.5 scenario. Here we argue that for realistic choices of phenomenological parameters, vortex clustering and type 1.5 behavior does occur in multiband chiral Ginzburg–Landau theories for Sr_2RuO_4 .

We consider a two-band chiral Ginzburg–Landau theory which incorporates the multiband nature of the superconductivity. In accordance with the discussion above, the superconducting gap function is taken to belong to the E_u representation of the tetragonal point group. This representation describes a chiral superconductor. The four complex components of the order parameter are related to the spin-triplet gap functions by $\mathbf{d}_a(\mathbf{k}) = [\psi_1^{(a)} f_{x,a}(\mathbf{k}) + \psi_2^{(a)} f_{y,a}(\mathbf{k})] \hat{z}$ where the a labels one of the two bands and the functions $f_{x,a}(\mathbf{k})$ and $f_{y,a}(\mathbf{k})$ share the same symmetry properties as k_x and k_y under the symmetry operations of the point group D_{4h} . In the units where $\hbar = 1, c = 1, m = 1$, the two-band

situation can be modeled as follows:

$$\begin{aligned} \mathcal{F} = & |\nabla \times \mathbf{A}|^2 + \\ & + \sum_{a=1,2} \left\{ \delta_a \left(|D_x \psi_1^{(a)}|^2 + \gamma_a |D_y \psi_1^{(a)}|^2 \right. \right. \\ & + |D_y \psi_2^{(a)}|^2 + \gamma_a |D_x \psi_2^{(a)}|^2 \left. \left. \right) \right. \\ & + 2\delta_a \gamma_a \text{Re} \left[(D_x \psi_1^{(a)})^* D_y \psi_2^{(a)} + (D_y \psi_1^{(a)})^* D_x \psi_2^{(a)} \right] \\ & + \beta_a \gamma_a \text{Re}(\psi_1^{(a)*} \psi_2^{(a)}) + \beta_a (2\gamma_a - 1) |\psi_1^{(a)}|^2 |\psi_2^{(a)}|^2 \\ & + \sum_{b=1,2} \left. \left. \left. \alpha_a |\psi_b^{(a)}|^2 + \frac{\beta_a}{2} |\psi_b^{(a)}|^4 \right\} \right. \right. \\ & + 2\nu \sum_{b=1,2} \text{Re} \left[\psi_b^{(1)*} \psi_b^{(2)} \right], \end{aligned} \quad (1)$$

where $\psi_b^{(a)}$ represent the superconducting components in the different bands, $a = 1, 2$ denotes the band index, $b = 1, 2$ denotes the two different components of each condensate. $\text{Re}[\]$ stands for real part of the expression in brackets. Each component of a given condensate is a complex function $\psi_a = |\psi_a| \exp\{i\varphi_a\}$. The gauge covariant derivative is $\mathbf{D} = \nabla + ie\mathbf{A}$ and $\mathbf{B} = \nabla \times \mathbf{A}$. The gauge coupling constant e is used to parametrize the penetration length of the magnetic field. This free energy is comprised of two free energies, one for each band, that are coupled through the vector potential \mathbf{A} and by the parameter ν . The free energies of each band are determined by weak coupling theory in the clean limit (both are reasonable assumptions for Sr_2RuO_4). No assumptions are made about the properties or geometry of the Fermi surface. The superconducting gap functions $f_{y,a}(\mathbf{k})$ are assumed to be given by the Fermi velocity components $v_x(\mathbf{k})$ and $v_y(\mathbf{k})$. This approximation provides the correct momentum dependence of the gap for the limiting cases of a purely cylindrical Fermi surface and a perfectly square Fermi surface.¹² The direct coupling of the bands through the sole parameter ν is also justified within a weak coupling theory. The phenomenological theory has nine parameters that require specification. Experiments place constraints on these parameters. In particular, one band is required to be passive and the other active. We assume that the γ -band is the active band and that the α/β bands give rise to a passive gap. This assumption is not critical, the results will be similar if we assume the other possibility.^{18,19,21} This assumption implies $\alpha_1 < 0$ and $\alpha_2 > 0$. Since the realization of type-1.5 state will be very similar for $\alpha_1 > 0$ and $\alpha_2 < 0$, without loss of generality we report numerical investigation of only the first scenario.

Additionally, for magnetic fields applied along the c -axis, the free energy should reproduce the experimentally determined ratio of H_{c2} and H_{c1} . Finally, weak coupling calculations show that $\gamma_1 > 1/3$ and $\gamma_2 < 1/3$ and consistency with the small observed anisotropy of the in-plane upper critical field requires that both γ_1 and γ_2 are close to $1/3$.³³

Equations of motion of the gauge field defines the supercurrent

$$\mathbf{J} = \sum_{a,b} \mathbf{J}_{(b)}^{(a)}, \quad (2)$$

where the contribution of each component of a given condensate is

$$\begin{aligned} J_{(1),x}^{(a)} &= \frac{e\delta_a}{2} \text{Im} \left[\psi_1^{(a)*} (D_x \psi_1^{(a)} + \gamma_a D_y \psi_2^{(a)}) \right] \\ J_{(1),y}^{(a)} &= \frac{e\delta_a \gamma_a}{2} \text{Im} \left[\psi_1^{(a)*} (D_y \psi_1^{(a)} + D_x \psi_2^{(a)}) \right] \\ J_{(2),x}^{(a)} &= \frac{e\delta_a \gamma_a}{2} \text{Im} \left[\psi_2^{(a)*} (D_x \psi_2^{(a)} + D_y \psi_1^{(a)}) \right] \\ J_{(2),y}^{(a)} &= \frac{e\delta_a}{2} \text{Im} \left[\psi_2^{(a)*} (D_y \psi_2^{(a)} + \gamma_a D_x \psi_1^{(a)}) \right], \end{aligned} \quad (3)$$

where Im stands for imaginary part.

Coalescence of vortex matter into clusters is investigated numerically by minimizing the free energy (1) within a finite element framework provided by the FreeFem++ library.³⁴ We investigated vortex matter in the model (1) for parameters which give characteristic length scales which are close to experimental estimates for Sr_2RuO_4 . We report the case $(\alpha_1, \beta_1) = (-10, 10)$, $\gamma_1 = 0.35$ and $\delta_1 = 1$. Parameters associated with the second condensate are $(\alpha_2, \beta_2) = (0.3, 1)$, $\gamma_2 = 0.25$ and $\delta_2 = 1$. The interband coupling is $\nu = 0.45$ and the electric charge $e = 1.8$. We also investigated a range of similar parameters to ensure that they give a similar picture (i.e. the parameter set does not correspond to any fine-tuned situation). For a general study how type-1.5 behavior is affected by interband coupling ν see Refs. 25–27, and 29. Note that, the models like (1) can have a Skyrmionic phase, where the vortices are unstable against a decay to Skyrmons.³⁵ We obtained stable vortex clusters in various type-1.5 regimes which are stable against a decay into Skyrmons. Fig. 1 shows a numerical solution for one such vortex cluster. We also find that Skyrmons can still exist in those regimes as metastable topological excitations, which are more energetically expensive than vortices.

Note that the experiments^{9,10,22} were performed at $T \ll T_c$. A microscopic approach is therefore required to get all aspects of the physics quantitatively correct since the Ginzburg–Landau model is quantitatively correct only for T near to T_c . However, under certain circumstances, a phenomenological Ginzburg–Landau model can qualitatively and quantitatively describe the long-range intervortex forces in the type-1.5 regime even at relatively low temperatures. This was shown in a two-band system with not too strong interband coupling and one passive band.²⁹ The physics that a GL-based approach fails to describe in the low temperature regime, is primarily associated with shorter-length scales such as the counterpart of Kramer–Pesch effect. Since in our study we are only interested in long-range intervortex forces (*i.e.* we do not consider the high-field regimes, where intervortex distance is short), the phenomenological GL

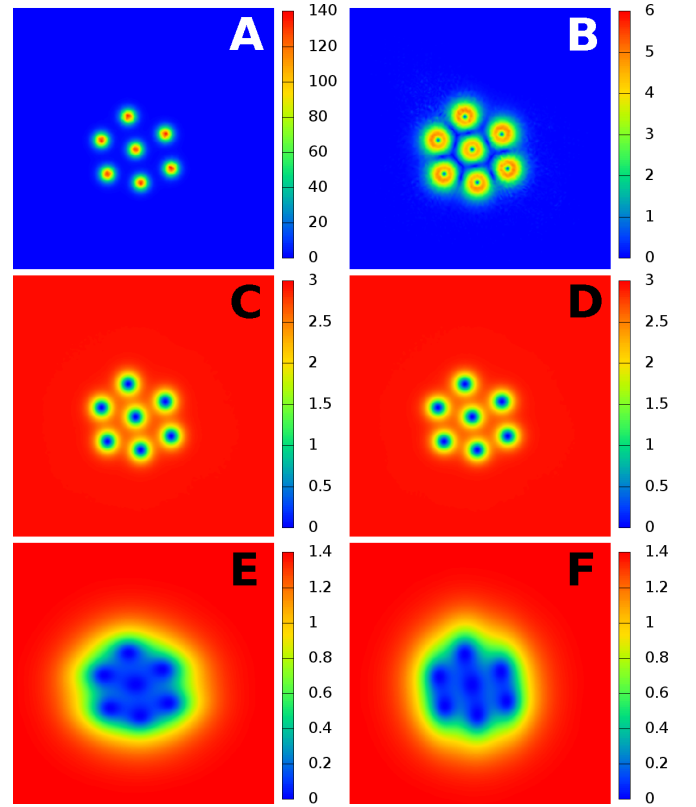


Figure 1. (Color online) – A vortex cluster obtained numerically by energy minimization from a dilute system of seven vortices. Displayed quantities are the magnetic field B_z on (A) and the total supercurrent (2) on (B). The densities of the first (*resp.* second) component of the condensate $\psi^{(1)}$, namely $|\psi_1^{(1)}|^2$ (*resp.* $|\psi_2^{(1)}|^2$), are shown on (C) (*resp.* (D)). The panels (E) (*resp.* (F)) show the densities of the first (*resp.* second) component of the condensate $\psi^{(2)}$, that is $|\psi_1^{(2)}|^2$ (*resp.* $|\psi_2^{(2)}|^2$). The figure demonstrates existence of several length scales associated with the density variations. The panels (E) (*resp.* (F)) show extended cores, the overlap of these cores leads to attractive intervortex forces.

approach still provides a qualitatively correct picture of that physics even at relatively low temperatures.

The experiments in Refs. 22, 10 and 23 obtain rather similar intervortex distances within the clusters. The typical intervortex distance is larger than their estimates of the London penetration length. Intervortex attraction is indeed achievable in type-1.5 regime at such length scales. The minimum of the intervortex interaction potential is determined not only by the length scales λ, ξ_1, ξ_2 but also by non-linear effects. Thus in a type-1.5 regime intervortex distance in a cluster could be substantially larger than the London penetration length scale. For example, the intervortex potential shown on Figure 2 in Ref. 26 corresponds to such a situation. It should be noted that all experiments observing vortex clusters (Refs. 9, 10, 22), are scanning SQUID or Hall experiments which probe magnetic field at a small distances over the sample’s surface. It should be kept in mind that such a

surface probe could in general overestimate the position of the minimum of the interaction potential, for vortices with nonmonotonic interactions. Indeed, near the surface, the long-range intervortex forces can be altered by the electromagnetic repulsion caused by the stray fields outside the sample (schematically shown in Fig. 2). Similarly, stray field physics affects the structure of normal domains in ordinary type-1 superconductors.³⁶

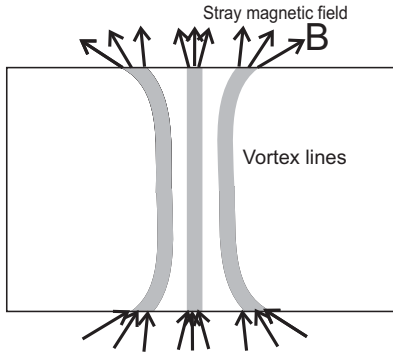


Figure 2. Even if vortices have attractive forces in the bulk, their segments near the surface can have long-range contributions to repulsive interaction due to the effects of demagnetization fields outside the sample. This is schematically shown on this figure. Thus a surface probe of a bulk sample can overestimate the position of the minimum in the intervortex potential. Also in case of a thin film, the stray fields can make intervortex distance larger.

The simplest origin of inhomogeneous vortex distributions are the pinning effects. And in fact in some of the samples, existence of preferential pinning areas were identified in the work of Curran *et. al.*,^{23,37} see also remark³⁸. However, in the experimental papers²² it was argued that the observed vortex clustering is not related to pinning. The layered structure of Sr_2RuO_4 leads to vortex stripes formation when in-plane field is applied. Therefore it is possible to move vortices by applying the in-plane component of the external magnetic field. Thus it is possible to assess this way, if the vortex clusters are artifacts of some local pinning landscape. In the Ref. 22 it was argued that the mobility of the vortex clusters in their samples is inconsistent with clustering due to a pinning scenario.

The distribution of the intervortex distance in several

samples with a relatively small number of vortices was analyzed in.²³ They found that it did not exhibit a clear peak at certain preferred intervortex distance, which was interpreted as being inconsistent with the type-1.5 scenario. We argue however that it does not necessarily contradict the type-1.5 scenario, for the following reasons. The shape of the vortex clusters in a certain subset of type-1.5 regimes is rather substantially affected by non-pairwise contributions to intervortex forces³⁰ (and also by dynamic and entropic aspects associate with it). This can affect the distribution of intervortex distances. Since the multiband model of Sr_2RuO_4 has four components, the non-pairwise contributions to intervortex forces could be relatively significant and produce variation in the shapes of vortex clusters. Due to these effects, it can be more difficult to get a distinguishable double-peak structure from vortex distributions in small samples like those studied in Ref. 23. Large samples with a larger number of vortices can yield a more conclusive answer. The absence of collapse to a single vortex cluster noticed in Refs. 22 and 10, also naturally arises in type-1.5 regime. Again it can originate in dynamic and entropic reasons and be enhanced by non-pairwise contributions to intervortex forces.³⁰ It can also be a result of demagnetization (stray fields) effects.

In conclusion, we have shown that vortex coalescence occurs in a realistic phenomenological model describing the multicomponent superconductivity in Sr_2RuO_4 . This provides an explanation for the vortex coalescence that was reported by several experimental groups. These experiments can be interpreted as demonstrating that Sr_2RuO_4 is a type-1.5 superconductor: *i.e.* it possess several coherence length: some longer than the London penetration length and some shorter. In order to firmly establish this interpretation, further experimental studies on the distribution of vortices are required.

We thank Peter Curran, Clifford Hicks, Simon Bending, Kam Moler and Victor Moshchalkov for useful correspondence. This work was supported by Knut and Alice Wallenberg Foundation through the Royal Swedish Academy of Sciences, Swedish Research Council and by the NSF CAREER Award No. DMR-0955902. DFA is supported by NSF grant DMR-0906655. The computations were performed on resources provided by the Swedish National Infrastructure for Computing (SNIC) at National Supercomputer Center at Linköping, Sweden.

¹ A. P. Mackenzie and Y. Maeno, *Rev. Mod. Phys.* **75**, 657 (May 2003).

² K. Ishida, H. Mukuda, Y. Kitaoka, K. Asayama, Z. Q. Mao, Y. Mori, and Y. Maeno, *Nature* **396**, 658 (Dec. 1998).

³ H. Murakawa, K. Ishida, K. Kitagawa, Z. Q. Mao, and Y. Maeno, *Phys. Rev. Lett.* **93**, 167004 (Oct. 2004).

⁴ G. M. Luke, Y. Fudamoto, K. M. Kojima, M. I. Larkin, J. Merrin, B. Nachumi, Y. J. Uemura, Y. Maeno, Z. Q.

Mao, Y. Mori, H. Nakamura, and M. Sigrist, *Nature* **394**, 558 (Aug. 1998).

⁵ J. Xia, Y. Maeno, P. T. Beyersdorf, M. M. Fejer, and A. Kapitulnik, *Phys. Rev. Lett.* **97**, 167002 (Oct. 2006).

⁶ K. D. Nelson, Z. Q. Mao, Y. Maeno, and Y. Liu, *Science* **306**, 1151 (2004).

⁷ F. Kidwingira, J. D. Strand, D. J. Van Harlingen, and Y. Maeno, *Science* **314**, 1267 (2006).

- ⁸ M. Matsumoto and M. Sigrist, *J. Phys. Soc. Jpn.* **68**, 994 (1999).
- ⁹ P. G. Björnsson, Y. Maeno, M. E. Huber, and K. A. Moler, *Phys. Rev. B* **72**, 012504 (Jul. 2005).
- ¹⁰ C. W. Hicks, J. R. Kirtley, T. M. Lippman, N. C. Koshnick, M. E. Huber, Y. Maeno, W. M. Yuhasz, M. B. Maple, and K. A. Moler, *Phys. Rev. B* **81**, 214501 (Jun. 2010).
- ¹¹ J. Jang, D. G. Ferguson, V. Vakaryuk, R. Budakian, S. B. Chung, P. M. Goldbart, and Y. Maeno, *Science* **331**, 186 (Jan. 2011).
- ¹² D. F. Agterberg, *Phys. Rev. Lett.* **80**, 5184 (Jun. 1998).
- ¹³ C. Bergemann, A. P. Mackenzie, S. R. Julian, D. Forsythe, and E. Ohmichi, *Advances in Physics* **52**, 639 (2003).
- ¹⁴ D. F. Agterberg, T. M. Rice, and M. Sigrist, *Phys. Rev. Lett.* **78**, 3374 (Apr. 1997).
- ¹⁵ M. E. Zhitomirsky and T. M. Rice, *Phys. Rev. Lett.* **87**, 057001 (Jul. 2001).
- ¹⁶ J. F. Annett, G. Litak, B. L. Györfy, and K. I. Wysokiński, *Phys. Rev. B* **66**, 134514 (Oct. 2002).
- ¹⁷ K. Deguchi, Z. Q. Mao, H. Yaguchi, and Y. Maeno, *Phys. Rev. Lett.* **92**, 047002 (Jan. 2004).
- ¹⁸ S. Raghu, A. Kapitulnik, and S. A. Kivelson, *Phys. Rev. Lett.* **105**, 136401 (Sep. 2010).
- ¹⁹ Y. Imai, K. Wakabayashi, and M. Sigrist, *Phys. Rev. B* **85**, 174532 (May 2012).
- ²⁰ P. E. C. Ashby and C. Kallin, *Phys. Rev. B* **79**, 224509 (Jun. 2009).
- ²¹ E. Taylor and C. Kallin, *Phys. Rev. Lett.* **108**, 157001 (Apr. 2012).
- ²² V. O. Dolocan, C. Veauvy, F. Servant, P. Lejay, K. Hasselbach, Y. Liu, and D. Mailly, *Phys. Rev. Lett.* **95**, 097004 (Aug. 2005); K. Hasselbach, V. Dolocan, P. Lejay, and D. Mailly, *Physica C* **460–462**, Part 1, 277 (2007).
- ²³ P. J. Curran, V. V. Khotkevych, S. J. Bending, A. S. Gibbs, S. L. Lee, and A. P. MacKenzie, *Phys. Rev. B* **84**, 104507 (Sep. 2011).
- ²⁴ A. Jacobs, *J. Low Temp. Phys.* **10**, 137 (1973); M. C. Leung and A. E. Jacobs, *ibid.* **11**, 395 (May 1973); M. C. Leung, *ibid.* **12**, 215 (Jul. 1973); U. Klein, *ibid.* **69**, 1 (1987).
- ²⁵ E. Babaev and J. M. Speight, *Phys. Rev. B* **72**, 180502 (2005); E. Babaev, J. Carlström, and M. Speight, *Phys. Rev. Lett.* **105**, 067003 (Aug. 2010).
- ²⁶ J. Carlström, E. Babaev, and M. Speight, *Phys. Rev. B* **83**, 174509 (May 2011).
- ²⁷ M. Silaev and E. Babaev, *Phys. Rev. B* **84**, 094515 (Sep. 2011).
- ²⁸ V. Moshchalkov, M. Menghini, T. Nishio, Q. H. Chen, A. V. Silhanek, V. H. Dao, L. F. Chibotaru, N. D. Zhigadlo, and J. Karpinski, *Phys. Rev. Lett.* **102**, 117001 (Mar. 2009); T. Nishio, V. H. Dao, Q. Chen, L. F. Chibotaru, K. Kadowaki, and V. V. Moshchalkov, *Phys. Rev. B* **81**, 020506 (Jan. 2010).
- ²⁹ M. Silaev and E. Babaev, *Phys. Rev. B* **85**, 134514 (Apr. 2012).
- ³⁰ J. Carlström, J. Garaud, and E. Babaev, *Phys. Rev. B* **84**, 134515 (Oct. 2011).
- ³¹ V. H. Dao, L. F. Chibotaru, T. Nishio, and V. V. Moshchalkov, *Phys. Rev. B* **83**, 020503 (Jan. 2011).
- ³² R. Geurts, M. V. Milošević, and F. M. Peeters, *Phys. Rev. B* **81**, 214514 (Jun. 2010).
- ³³ D. F. Agterberg, *Phys. Rev. B* **64**, 052502 (Aug. 2001).
- ³⁴ F. Hecht, O. Pironneau, A. Le Hyaric, and K. Ohtsuka, *The Freefem++ manual* (2007) www.freefem.org
The integration domain, is discretized using an algorithm based on Delaunay–Voronoi triangulation and each function is decomposed on a piecewise quadratic basis. The discrete version of Eq. (1) is then minimized with respect to all degrees of freedom, for a starting configuration with an initial guess for N vortices using a Non-Linear Conjugate Gradient scheme.
- ³⁵ J. Garaud and E. Babaev (Jan. 2012), [arXiv:1201.2946](https://arxiv.org/abs/1201.2946).
- ³⁶ P. de Gennes, *Superconductivity of metals and alloys* (Perseus Books, 1999).
- ³⁷ P. J. Curran and S. J. Bending, *Private communication*.
- ³⁸ Note that in chiral superconductors vortex pinning can arise not only from sample inhomogeneities but also due to vortex interaction with pinned domain walls between different chiral domains^{35,39}.
- ³⁹ M. Ichioka, Y. Matsunaga, and K. Machida, *Phys. Rev. B* **71**, 172510 (May 2005); V. Vakaryuk, *ibid.* **84**, 214524 (Dec. 2011); D. G. Ferguson and P. M. Goldbart, *Phys. Rev. B* **84**, 014523 (Jul. 2011).